

## Observations of the 2.2- $\mu$ m Emission from the Halo of NGC 4244 at Large Galactocentric Distances

J. W. BERGSTROM, R. D. GEHRZ, AND T. J. JONES

Department of Astronomy, School of Physics and Astronomy, University of Minnesota, Minneapolis, Minnesota 55455  
Electronic mail: rdg@ast1.spa.umn.edu, tj@ast1.spa.umn.edu

Received 1992 March 4; accepted 1992 May 1

**ABSTRACT.** We report observations of 2.2- $\mu$ m emission from the halo of the edge-on spiral galaxy NGC 4244. These observations were made at larger radii from the center of the galaxy and with a smaller beam than reported in previous studies. The emission we detected is consistent with the de Vaucouleurs  $r^{1/4}$  law, and the mass-to-light ratio given by our measurements at 2.2  $\mu$ m is in good agreement with previous results. Our data reveal no evidence for a massive halo of cool objects.

### 1. INTRODUCTION

Dark matter, as defined by Binney and Tremaine (1987), is “any form of matter whose existence is inferred solely from its gravitational effects.” The determination of its nature is one of the foremost unresolved questions in extragalactic astronomy. Near-infrared measurements are capable of testing the hypothesis that dark matter in galactic halos is in the form of low-mass stars and substellar objects (brown dwarfs) with effective temperatures in the range approximately 300–1500 K and emission maxima between 2 and 10  $\mu$ m (see Hegyi and Olive 1986, hereafter referred to as HO). These objects are sufficiently cool that they will escape detection in the visible region, but emission from an extended halo of these objects that is ten times as massive as the visible galactic disk should be detectable at 2.2  $\mu$ m ( $K$  band). Searches at longer wavelengths closer to the Planckian maximum for these objects are limited by the thermal background radiation from the telescope and atmosphere, while those at shorter wavelength are compromised by OH airglow emission and decreasing source brightness. The  $K$  band offers a good compromise between source and background brightness for ground-based studies.

A recent review of observational searches for massive dark halos in spiral galaxies (Van der Kruit 1987) lists several edge-on candidates that have been studied in the visible and near infrared wavelengths. These searches have virtually eliminated main-sequence stars as a major constituent of massive galactic halos (e.g., Hohlfeld and Krumm 1981; Boughn et al. 1981). The most recent search was conducted by Skrutskie et al. (1985; hereafter referred to as SSB), who examined the three late-type spiral galaxies NGC 2683, NGC 4244, and NGC 5907. The primary advantage of conducting such searches using late-type spiral galaxies is that they do not have a large (visually bright) central bulge component in comparison with the total mass of the galaxy inferred from rotation curves measurements. In this paper we report new results on the halo of NGC 4244 obtained using a novel beam-switching technique. These results extend the 2.2- $\mu$ m observations of the halo to larger galactocentric distances and with a smaller beam than studied by SSB. The advantage of using a

smaller beam is a lower chance of contamination by a bright (but optically invisible) star in the beam and less effect of the surface brightness gradient in the halo on the effective location of the radial position of the beam.

### 2. OBSERVATIONAL TECHNIQUE

Previous studies have been confined to distances of less than 2' from the centers of galaxies. The computer telescope control and data-acquisition system at the Wyoming Infrared Observatory afforded us the opportunity of obtaining long-term stability in the tracking and positioning of the telescope so that we could consider a modified beam-switching technique to detect halo emission from edge-on spiral galaxies at large galactocentric distances. The technique tests for emission from portions of the halo that are symmetric about the nucleus, but separated by large distances on the sky in such a way that the galactic plane and bulge do not contaminate the measurement.

Figure 1 illustrates the method of beam switching we devised for background subtraction in this experiment. Normal infrared beam-switching photometry is accomplished by placing the reference beam alternately to either side of the source beam by a fixed amount called the “throw” that is generated by rocking the secondary mirror of the telescope. Because there are physical limitations on the amplitude and direction of the throw that can be achieved by most rocking secondary mirrors [about 3' in the north-south direction on the Wyoming Infrared Observatory (WIRO) system], the normal beam-switching procedure will result in significant contamination from the inner halo and galactic disk in one of the reference beams. Our technique is to alternately integrate on geometrically symmetric “source” positions above and below the galactic disk that place the corresponding reference beams away from the galactic disk. Assuming, as do virtually all existing models of the halo mass distribution, that the dark halo is spherically symmetric, beam switching in this fashion will produce a signal equal to the average of those generated at the two source positions. Specifically, as shown in Fig. 1(a), the signal  $S$  is given by

$$S = 2(G_1 - G_2) + (B_{N1} + B_{S1}) - (B_{N2} + B_{S2}) \sim 2(G_1 - G_2), \quad (1)$$

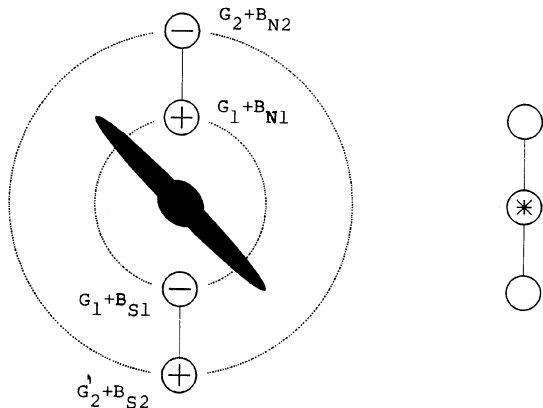


FIG. 1—Our method (left) of chopping and offsetting the telescope beam to measure the galaxy halo with a limited chopper throw, and (right) the conventional chopping method for point sources. The galaxy contribution is indicated by the letter  $G$  and the telescope and sky background is indicated by the letter  $B$ .

where  $G_{1,2}$  are the galactic-halo signals at positions 1 and 2, respectively, and  $B_{N1,N2,S1,S2}$  are the sky background signals at the two north and two south positions, respectively. The telescope computer control system enabled us to drive the telescope rapidly and accurately between positions  $G_1$  and  $G_2$  to accomplish this measurement routinely for many hours of integration time.

If the surface brightness of the halo is decreasing as a function of galactocentric radius, the technique will result in a positive signal, and the correction to be applied for halo contamination in the reference beam will depend on the surface brightness distribution. For example, if the halo surface brightness decreases as  $r^{-1}$ , the average source strength of the galactic halo at  $G_1$  will be given by

$$G_1 = \frac{4T(G_1 - G_2)}{(4T - D)}, \quad (2)$$

where  $T$  is the throw in arcseconds and  $D$  is the beam diameter in arcseconds (see Gehrz and Ney 1992). Thus, any positive detections obtained by this technique provide, at a minimum, evidence for gradients in the surface brightness distribution of the halo.

Our  $2.2\text{-}\mu\text{m}$  ( $K$ ) observations of NGC 4244 were obtained on 1989 March 15 UT and 1989 April 13–14 UT on the 234-cm telescope of the WIRO. All of the measurements were made using a multiple-aperture, large-beam,  $1\text{--}5\text{-}\mu\text{m}$  InSb photometer developed at the University of Minnesota by Bergstrom (1989, 1990). We used a zero-magnitude flux of  $3.92 \times 10^{-14}$  for the  $K$  filter to determine the flux calibration for our observations. The measured sensitivity of the detector and electronics for a chopping frequency of 7.5 cycles per second was  $5 \times 10^{-17} \text{ W Hz}^{-1/2}$  with the detector blanked off (zero magnitude corresponds to  $2.0 \times 10^{-10} \text{ W}$  on the detector). The system was background limited at  $K$  on the Wyoming telescope for apertures larger than  $3''$  in diameter. Our experiment employed an aperture diameter of  $26''.7$  and a chopper throw of  $104''$  between the source and reference beams.

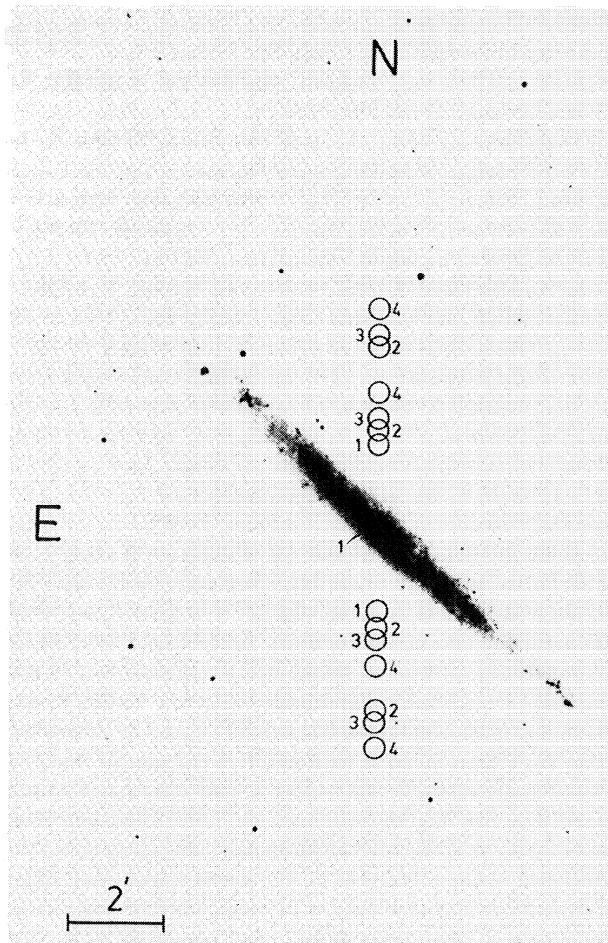


FIG. 2—Photograph of NGC 4244 with circles drawn to indicate the location of several beams for each of the four galactocentric radii measured (original photograph from Sandage and Bedke 1988).

### 3. GALAXY AND REFERENCE FIELD SELECTION

A good use of the observing technique described above was afforded by the Scd galaxy NGC 4244 because of the orientation of its edge-on disk on the sky (see Fig. 2) and the relative paucity of foreground stars that could cause contamination in the reference beams. We will assume, as did SSB, that the rotation curve is flat well beyond the Holmberg radius, although Bosma (1981) had suggested that the rotation curve was falling.

Figure 2 shows the positions in the halo of NGC 4244 that we selected for the placement of our  $26''.7$  beams. The beam positions were initially chosen to avoid obvious contamination by foreground stars in either the source or reference beams by examination of the POSS O plate. Any star brighter than  $K = +16$  mag, but too faint in the visible to be seen on the POSS plates, could be detected with our InSb system after just a few minutes. In one instance we had to adjust our initial beam positions by offsetting the telescope by a few arcseconds to eliminate the source of confusion.

There remains a small but finite probability that faint unidentified foreground stars were present in one or more

TABLE 1  
Observed Surface Brightness

Radius (arcsec)	Correction factor	Corrected for an $r^{1/4}$ Law		$\mu_K$ (mag arcsec $^{-2}$ )
		Corr. mean (W cm $^{-2}$ $\mu$ m $^{-1}$ )	Error (W cm $^{-2}$ $\mu$ m $^{-1}$ )	
0	1.00	$1.55 \times 10^{-18}$	$7.5 \times 10^{-20}$	17.88
125	1.31	$2.2 \times 10^{-20}$	$6.5 \times 10^{-21}$	22.49
140	1.35	$5.2 \times 10^{-21}$	$4.3 \times 10^{-21}$	...
173	1.44	$3.4 \times 10^{-21}$	$3.3 \times 10^{-21}$	...
Radius (arcsec)	Correction factor	Corrected for an $r^{-1}$ Law		$\mu_K$ (mag arcsec $^{-2}$ )
		Corr. mean (W cm $^{-2}$ $\mu$ m $^{-1}$ )	Error (W cm $^{-2}$ $\mu$ m $^{-1}$ )	
0	1.00	$1.55 \times 10^{-18}$	$7.5 \times 10^{-20}$	17.88
125	2.20	$3.7 \times 10^{-20}$	$1.1 \times 10^{-20}$	21.93
140	2.35	$9.1 \times 10^{-21}$	$7.6 \times 10^{-22}$	...
173	2.66	$6.2 \times 10^{-21}$	$6.0 \times 10^{-21}$	...

of the beams. We used a model for the 2.2- $\mu$ m source counts in the Milky Way (Garwood and Jones 1987) that included M dwarfs to estimate the probability of obtaining erroneous results by our technique due to faint unidentified infrared stars not visible on the POSS plates. No attempt was made to estimate the effect of background extragalactic sources since their density is very low and no detailed model regarding their spatial distribution exists. The predicted number of  $K$  sources brighter than 25th magnitude is  $\sim 0.7$  in the solid angle subtended by the four 26"7 beams used in our technique. However, single objects fainter than 18th magnitude falling within the beams would result in an error of less than  $0.8\sigma$  for the integration times used in our study. Stars brighter than 16th magnitude were eliminated from the fields as described above. Thus, only stars between 16th and 18th magnitude at  $K$  prove to be a serious potential source of contamination. The Garwood and Jones model predicts that the probability that one such object will fall within four beam diameters is less than 5%. We conclude that contamination by foreground stars is unlikely to have a significant effect on our data.

#### 4. ANALYSIS AND RESULTS

The results presented in Table 1 are based on data taken on three nights when the sky emission was low and stable, and at positions on the sky where our data were not subject to obvious contamination by unidentified stars. Only once was it necessary to change the chop length to avoid contamination of a field star (which showed up immediately within a few integrations, but was not visible on the Polar Sky Prints). On nights when airglow was strong, the entire night was discarded as a result. In essence, the reported results represent the lowest signal levels we were able to measure.

Each integration, or beam difference, was 20 s, 10 s in each beam with beam switching taking place every 20 s (commonly referred to as ABBA beam switching). There was a built-in pause of 2 s after a beam switch to allow the telescope to move and settle (typically taking 1 s). A total of 32 integrations (640 s) were taken before checking the

telescope pointing or measuring the standard. One set of 32 integrations constituted 1 observation. The result for  $r = 125''$  is the average of 4 observations and the result for  $r = 140''$  is the average of 6 observations. For  $r = 173''$ , 23 observations were made over 2 nights for a total of 4 hr of integration time. One of the 23 observations was discarded due to voltage spikes in the instrumentation. For  $r = 173''$ , the average of the standard deviations for each of the observations (obtained from the 32 individual 20-s integrations) was within 5% of  $\sqrt{32}$  times the standard deviation computed from the distribution of the 22 observations. This indicates that the sky background noise was reasonably steady over the observing time and that individual observations can be considered to have the same parent distribution.

A correction for the finite chopping amplitude is required because the chopping amplitude was exceeded by the size of the galactic halo. Thus, halo signal in the reference beam is subtracted from the signal in the main beam as if it were a sky background. Determination of the correction to the measured difference signal needed to obtain the signal in the main beam requires knowledge of the radial gradient in the surface brightness of the halo. We considered two cases for the radial dependence of the halo surface brightness. First, we used the well-known de Vaucouleurs  $r^{1/4}$  law (de Vaucouleurs 1959) which was normalized to the inner halo surface brightness distribution given by SSB. The best fit was obtained by offsetting the SSB data by  $10''$  in the minor axis direction to provide symmetry with the galactic center. Considering that SSB's beam was  $48''$  in diameter, this slight asymmetry suggested by their data is probably not significant. We found that a good fit to the data under these assumptions was given by

$$\mu(r) = 8.325 \left[ \left( \frac{r}{r_e} \right)^{1/4} - 1 \right] + C_1, \quad (3)$$

where  $\mu(r)$  is the surface brightness distribution in K mag arcsec $^{-2}$ ,  $r_e = 140$  arcsec is the effective radius, and  $C_1 = 23.05$  is a constant offset level equal to the surface brightness at  $r = r_e$ . Given the position in the halo and the chop amplitude, this curve fit can be used to estimate to first order the reduction in signal and the corresponding correction factor to the measured difference signal in order to obtain the full signal from the halo.

The second form of the radial brightness distribution we considered was a simple  $r^{-1}$  law. For this brightness distribution the flux falls off more slowly with distance from the nucleus than for the de Vaucouleurs law. Consequently, there is a larger flux present in the reference beam and a larger correction must be made to obtain the true flux [see Eq. (2)]. The results for the  $r^{-1}$  case are also given in Table 1.

In our analysis, we have assumed that the halo distribution is azimuthally symmetric. Under this assumption, we can combine the SSB detections obtained along a line perpendicular to the plane of the galaxy with our observations taken along a line oriented at  $45^\circ$  to the plane of the galaxy. Figure 3 plots the data from SSB and our data from Table 1. The top panel in Fig. 3 plots our data reduced

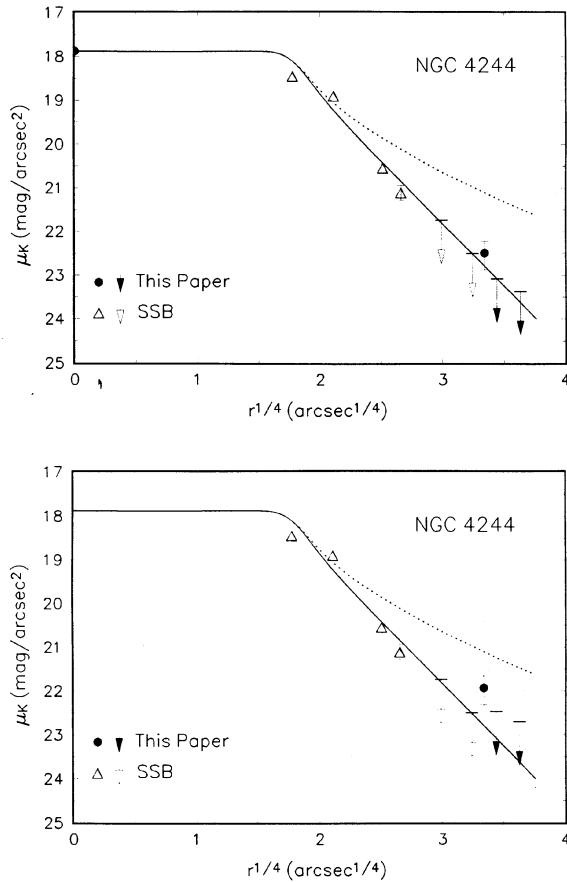


FIG. 3—Top panel: Radial surface-brightness distribution of NGC 4244. The solid circles and arrows are our data, corrected assuming a halo surface brightness that follows a de Vaucouleurs  $r^{1/4}$  spheroid. The solid line corresponds to an  $r^{1/4}$  law, convolved with our beam, and normalized to the data point at the nucleus. The dashed line is an  $r^{-1}$  law also convolved with our beam and normalized to the data at  $r=0$ . The open triangles and arrows are observations from SSB. Bottom panel: Same as above, except our observations were reduced assuming an  $r^{-1}$  law for the halo surface brightness.

with the assumption of an  $r^{1/4}$  law, and the bottom panel plots the data assuming an  $r^{-1}$  law. The solid line in both figures is an  $r^{1/4}$  law, convolved with our beam. The dashed line is the  $r^{-1}$  law, also convolved with our beam. The overall level of the two model lines were normalized to the data point at the nucleus.

As seen in Fig. 3, if the data are reduced assuming a simple  $r^{1/4}$  spheroid, the observations are entirely consistent with this assumption. The simplest interpretation of our results is that the halo of NGC 4244 as seen at  $2.2 \mu\text{m}$  behaves like a normal de Vaucouleurs spheroid out to a radius of 200 arcsec. In both figures the observations at large radii fall well below the  $r^{-1}$  law. In the bottom panel, the addition of an  $r^{-1}$  component onto the  $r^{1/4}$  spheroid beginning at a radius of about 50 arcsec is not ruled out by our observations. Such a composite radial profile is, however, inconsistent with the SSB data at large radii.

## 5. DISCUSSION

The mass-to-light ( $M/L$ ) ratio in the  $K$  band at a radius of 2.2 kpc for NGC 4244 was estimated by SSB to be 33 on the basis of their data, which extended to galactocentric radii of  $123''$ . For comparison, we will assume the same values as did SSB for the maximum rotation velocity  $V_{\text{max}}$  ( $110 \text{ km s}^{-1}$ ) and distance  $D$  (3.7 Mpc). These values are within 10% of other published results (e.g., Sancisi 1976; Bosma 1981; and Huchtmeier and Seiradakis 1985). SSB consider the case where a dominant spherically symmetric halo produces the flat rotation curve. Assuming a constant  $M/L$  ratio, this implies that the surface brightness of this massive spheroid (if it is luminous) would be proportional to  $r^{-1}$ .

A flat rotation curve for a spherically symmetric mass distribution gives  $M(r) = (V_{\text{max}}^2 r)/G$  where  $M(r)$  is defined by the integrating  $dM/dr = 4\pi r^2 \rho(r)$ . It can be shown that  $\rho(r)$  is given by

$$\rho(r) = \frac{V_{\text{max}}^2}{4\pi r^2 G}, \quad (4)$$

which can be integrated along the line of sight through the spherically symmetric halo to obtain the mass column-density distribution  $\Sigma(r)$ . This result can be compared to the measured surface brightness distribution [Eq. (3) for example]. We obtain

$$\Sigma(r) = \frac{V^2}{4rG} = 5.8 \times 10^4 \frac{V_{\text{max}}^2}{r(\text{kpc})} M_{\odot} \text{ kpc}^{-1}. \quad (5)$$

For NGC 4244, in the spherical halo,

$$\Sigma(r) = \frac{7.0 \times 10^8}{r(\text{kpc})} M_{\odot} \text{ kpc}^{-1}. \quad (6)$$

At a galactocentric radius of 3.1 kpc ( $173''$ ),  $\Sigma(r) = 2.3 \times 10^8 M_{\odot} \text{ kpc}^{-1}$ . The  $3\sigma$  upper limit (above zero, not above the mean) to the surface brightness at this radius is  $23.32 \text{ K mag arcsec}^{-2}$  (Table 1). Assuming the absolute  $K$  magnitude of the sun is  $M_{\odot K} = 3.41$ , the observed surface brightness at this position is  $\mu(3.1 \text{ kpc}) = 1500 L_{\odot K} \text{ arcsec}^{-2} = 4.7 \times 10^6 L_{\odot K} \text{ kpc}^{-2}$ . For the mass-to-light ratio we have

$$(M/L)_r = \frac{\Sigma(r)}{\mu(r)}. \quad (7)$$

Therefore, the  $3\sigma$  lower limit for the mass-to-light ratio  $M_{\odot}/L_{\odot K}$  at 3.1 kpc is 49, which is in good agreement with the value derived by SSB at 2.2 kpc (SSB used an upper limit of  $\langle x \rangle + 3\sigma$ ).

An  $r^{-1}$  surface brightness curve is also shown in Fig. 3. Because the measured results are falling faster than  $r^{-1}$ , using this relation to extrapolate the surface brightness to larger radii would obviously overestimate the luminosity at larger radii, and underestimate the  $M/L$  ratio there. However, if the rotation curve remains flat at larger radii, then the surface mass density must continue to fall off only as  $r^{-1}$ . Thus, the value of 45 would appear to be a lower limit to the  $M/L$  ratio of an extended halo.

This result relies on the assumption that the rotation curve (which is measured in the disk) is strongly influenced by the hypothesized massive halo at galactocentric radii in the range of our observations. The sensitivity of our IR measurement is not sufficient to approach the Holmberg radius; in fact, the largest radius at which we have measurements (3.1 kpc) is near the point where the rotation curve flattens. If, at 3.1 kpc, the disk mass makes a substantial contribution to the measured rotation curve velocity, then the contribution of the spheroid to the mass density within this radius must be reduced from our estimate. Essentially, this means reducing the value for  $V_{\max}$  in Eq. (6), and correspondingly reducing the value we have derived for  $M/L$ .

The measured  $M/L$  ratio can be compared with observations for various interesting objects and populations proposed for galactic halos. For example, the  $M/L$  ratio for a typical M5 dwarf and for the very low-mass star VB 10 are 9.6 and  $35 M_{\odot}/L_{\odot K}$  respectively (van der Kruit 1987). Thus, if there were a massive halo with an  $r^{-1}$  surface mass dependence, its composition is unlikely to have a major fraction of its mass in hydrogen burning stars. In fact, HO computes  $M/L$  at  $K$  in solar units as a function of the slope  $x$ , of the initial mass function (IMF). The ratio is only slightly dependent on the assumption of the minimum mass for substellar objects. For our observed  $M/L$  lower limit of 45, the results of HO indicate  $x > 1.8$  which is not at all consistent with observed populations. For example, globular clusters and elliptical galaxies can be fitted by  $x < 1.35$  (Aaronson et al. 1978; Frogel et al. 1980) and other more restrictive populations with  $x < 1$  have been found (see Mihalas and Binney 1981; HO). In the final analysis, the fact that our observations are most consistent with a normal de Vaucouleurs spheroid, suggests that the population of objects shining at  $2.2 \mu\text{m}$  in the halo at a radius of 3.1 kpc in NGC 4244 are normal halo stars.

## 6. SUMMARY

We have made  $K$ -band measurements of the halo emission from the edge-on spiral galaxy NGC 4244 40% further in galactocentric radius and with a smaller beam than

previous studies. No evidence was found for a massive luminous halo. The observed surface-brightness distribution is consistent with de Vaucouleur's  $r^{-1/4}$  law expected for a conventional halo population of normal stars. Our results support the view that the constituents of galactic halos, assuming that dynamical arguments demand their existence, must be very subluminescent.

We are grateful to D. Hegyi and K. Olive, who encouraged us to undertake this project, for useful discussions that helped to define our observational strategy. The Infrared Group of the University of Minnesota was supported by the National Science Foundation, the United States Air Force, NASA, and the Graduate School of the University of Minnesota.

## REFERENCES

- Aaronson, M., Cohen, J. G., Mould, J., and Malkan, M. 1978, *ApJ*, 223, 824
- Bergstrom, J. W. 1989, *Proc. SPIE*, 973, 278
- Bergstrom, J. W. 1990, Thesis, University of Minnesota
- Binney, J., and Tremaine, S. 1987, in *Galactic Dynamics* (Princeton, Princeton University Press), p. 589
- Bosma, A. 1981, *AJ*, 86, 1825
- Boughn, S. P., Saulson, P. R., and Selder, M. 1981, *ApJ*, 250, L15
- de Vaucouleurs, G. 1959, in *Handbuch der Physik*, Vol. 53, ed. S. Flugge (Berlin, Springer), p. 311
- Frogel, J. A., Persson, S. E., and Cohen, J. G. 1980, *ApJ*, 240, 785
- Garwood, R., and Jones, T. J. 1987, *PASP*, 99, 453
- Gehrz, R. D., and Ney, E. P. 1992, *Icarus*, submitted
- Hegyi, D. J., and Olive, K. A. 1986, *ApJ*, 303, 56 (HO)
- Hohlfeld, R. G., and Krumm, N. 1981, *ApJ*, 244, 476
- Huchtmeier, W. K., and Seiradakis, J. H. 1985, *A&A*, 143, 216
- Mihalas, D., and Binney, J. 1981, in *Galactic Astronomy—Structure and Kinematics* (San Francisco, Freeman), p. 231
- Sancisi, R. 1976, *A&A*, 53, 159
- Skrutskie, M. F., Shure, M. A., and Beckwith, S. 1985, *ApJ*, 299, 303 (SSB)
- Van der Kruit, P. C. 1987, in *IAU Symp.*, No. 117, *Dark Matter in the Universe*, ed. J. Kormendy and G. R. Knapp (Dordrecht, Reidel), p. 415